AMERICAN SOCIETY FOR MICROBIOLOGY | Journal of Virology®

PATHOGENESIS AND IMMUNITY

Mutations in the Neuraminidase-Like Protein of Bat Influenza H18N11 Virus Enhance Virus Replication in Mammalian Cells, Mice, and Ferrets

Gongxun Zhong,[a] Shufang Fan,[a] Masato Hatta,[a] Sumiho Nakatsu,[b] Kevin B. Walters,[a] Tiago J. S. Lopes,[a] Jessica I-Hsuan Wang,[b] Makoto Ozawa,[a] Alexander Karasin,[a] Yan Li,[c] Suxiang Tong,[c] Ruben O. Donis,[d] Gabriele Neumann,[a] Yoshihiro Kawaoka[a,b]

[a]Department of Pathobiological Sciences, School of Veterinary Medicine, University of Wisconsin—Madison, Madison, Wisconsin, USA
[b]Division of Virology, Department of Microbiology and Immunology, Institute of Medical Science, University of Tokyo, Tokyo, Japan
[c]Division of Viral Diseases, National Center for Immunization and Respiratory Diseases, CDC, Atlanta, Georgia, USA
[d]Influenza Division, National Center for Immunization and Respiratory Diseases, CDC, Atlanta, Georgia, USA

ABSTRACT To characterize bat influenza H18N11 virus, we propagated a reverse genetics-generated H18N11 virus in Madin-Darby canine kidney subclone II cells and detected two mammal-adapting mutations in the neuraminidase (NA)-like protein (NA-F144C and NA-T342A, N2 numbering) that increased the virus titers in three mammalian cell lines (i.e., Madin-Darby canine kidney, Madin-Darby canine kidney subclone II, and human lung adenocarcinoma [Calu-3] cells). In mice, wild-type H18N11 virus replicated only in the lungs of the infected animals, whereas the NA-T342A and NA-F144C/T342A mutant viruses were detected in the nasal turbinates, in addition to the lungs. Bat influenza viruses have not been tested for their virulence or organ tropism in ferrets. We detected wild-type and single mutant viruses each possessing NA-F144C or NA-T342A in the nasal turbinates of one or several infected ferrets, respectively. A mutant virus possessing both the NA-F144C and NA-T342A mutations was isolated from both the lung and the trachea, suggesting that it has a broader organ tropism than the wild-type virus. However, none of the H18N11 viruses caused symptoms in mice or ferrets. The NA-F144C/T342A double mutation did not substantially affect virion morphology or the release of virions from cells. Collectively, our data demonstrate that the propagation of bat influenza H18N11 virus in mammalian cells can result in mammal-adapting mutations that may increase the replicative ability and/or organ tropism of the virus; overall, however, these viruses did not replicate to high titers throughout the respiratory tract of mice and ferrets.

IMPORTANCE Bats are reservoirs for several severe zoonotic pathogens. The genomes of influenza A viruses of the H17N10 and H18N11 subtypes have been identified in bats, but no live virus has been isolated. The characterization of artificially generated bat influenza H18N11 virus in mammalian cell lines and animal models revealed that this virus can acquire mammal-adapting mutations that may increase its zoonotic potential; however, the wild-type and mutant viruses did not replicate to high titers in all infected animals.

KEYWORDS bat influenza, H18N11, NA, replication

Influenza A viruses of the H1 to H16 and N1 to N9 subtypes are maintained in wild waterfowl (1, 2) but can cause zoonotic events. In 2012 and 2013, the genomes of two novel influenza A virus subtypes (the H17N10 and H18N11 subtypes) were discovered

Citation Zhong G, Fan S, Hatta M, Nakatsu S, Walters KB, Lopes TJS, Wang JI-H, Ozawa M, Karasin A, Li Y, Tong S, Donis RO, Neumann G, Kawaoka Y. 2020. Mutations in the neuraminidase-like protein of bat influenza H18N11 virus enhance virus replication in mammalian cells, mice, and ferrets. J Virol 94: e01416-19. https://doi.org/10.1128/JVI.01416-19.

Editor Stacey Schultz-Cherry, St. Jude Children's Research Hospital

Address correspondence to Gabriele Neumann, gabriele.neumann@wisc.edu, or Yoshihiro Kawaoka, yoshihiro.kawaoka@wisc.edu.

Received 30 August 2019
Accepted 25 November 2019
Accepted manuscript posted online 4 December 2019
Published 14 February 2020

in bats in South America (3, 4), raising concerns that viruses of these subtypes may infect humans. No infectious viruses were isolated from the original bat samples (3, 4).

Some of the bat influenza virus proteins are functionally similar to or compatible with their counterparts in canonical influenza A viruses. The ribonucleoprotein (RNP) complex (composed of the polymerase and NP proteins) of bat influenza viruses showed polymerase activity *in vitro* (3, 5, 6). The N-terminal domain of the H17N10 PA protein possesses endonuclease activity comparable to that of canonical influenza A viruses (7). The NS1 proteins of bat influenza viruses bind double-stranded RNA and antagonize host innate immunity, similar to the findings for established influenza A virus NS1 proteins (8, 9). Moreover, the H17N10 virus M gene is compatible with that of canonical influenza A viruses (10).

The viral surface glycoproteins, hemagglutinin (HA) and neuraminidase (NA), play critical roles in the life cycle of influenza viruses. For influenza A viruses of the H1 to H16 subtypes, HA is responsible for virus binding to sialic acid-containing receptors on host cells (11–13), whereas NA cleaves the sialic acid from the receptors to release progeny viruses from infected cells (14–16). The activities of these two viral proteins must be balanced for efficient virus replication (17–24). The H17 and H18 bat influenza virus HA proteins bear some structural similarity to H1 to H16 HAs, although the shape of their receptor-binding pockets differs from that of the receptor-binding pockets of the H1 to H16 HAs (4); moreover, the amino acids in the presumed receptor-binding site of the H17 and H18 HAs are acidic, making an interaction with negatively charged sialic acids unlikely. In line with this finding, the H17 and H18 HA proteins did not interact with >600 sialic acid-containing glycan structures tested in glycan arrays (4, 25). These data suggest that the cellular receptors of bat influenza viruses differ from those of conventional influenza viruses. In fact, Karakus et al. (26) recently reported that major histocompatibility complex class II proteins serve as receptors for bat influenza viruses. The N10 and N11 NA-like proteins bear some structural similarity to their N1 to N9 counterparts but lack the putative sialic acid-binding sites and do not possess sialidase activity (4, 27, 28). Currently, the role of the N10 and N11 NA-like proteins in bat influenza virus replication is not understood.

Moreira et al. (29) tested more than 30 cell lines with a pseudotyped vesicular stomatitis virus (VSV) expressing H17 or H18 HA and found that Madin-Darby canine kidney subclone II (MDCK II) cells, but not the commonly used MDCK cells, were susceptible to the pseudotyped viruses. The identification of cell lines that are sensitive to infection with H17 and H18 viruses opened the door for the generation of H17N10 and H18N11 viruses by reverse genetics (29) and their further characterization. Here, we generated bat influenza H18N11 virus by reverse genetics and detected mammal-adapting amino acid changes in the NA-like protein that emerged during passages in MDCK II cells; these mutations enhanced the replicative ability of the H18N11 virus in cultured cells and broadened their organ tropism in mice and ferrets.

RESULTS

H18N11 virus generation and adaptation to MDCK II cells. The full-length genomic sequence of a novel influenza A virus, A/flat-faced bat/Peru/033/2010 (H18N11) virus, was recovered from a rectal swab sample from a South American bat (4); however, no infectious virus was isolated from the bat. To characterize the bat influenza virus, we cloned its genomic cDNA into vectors for influenza virus reverse genetics as described previously (30). Briefly, the eight viral cDNAs of H18N11 virus were cloned into viral RNA (vRNA) transcription plasmids between the human RNA polymerase I promoter and the mouse RNA polymerase I terminator. Viral cDNAs of the PB2, PB1, PA, and NP segments were cloned into a eukaryotic protein expression plasmid (pCAGGS) under the control of the chicken β-actin promoter (31). The plasmids for viral RNA transcription and protein expression were mixed and transfected into 293T cells. The cell culture supernatant derived from transfected 293T cells was inoculated into mammalian cells as described below.

Moreira et al. (29) reported that MDCK II cells (which consist of subclones of MDCK cells that predominate after multiple passages [32]) were susceptible to H18N11 virus. Here, we confirmed that MDCK II cells supported the replication of H18N11 virus; however, the virus replicated inefficiently, based on indirect immunofluorescence analysis. In MDCK.2 cells (which consist of a single population of cells that is highly susceptible to various influenza viruses [33]), H18N11 virus replication was substantially restricted, with only a few cells expressing viral protein. No H18N11 virus replication was detected in MDCK cells, as previously reported (29).

Moreira et al. (29) also reported that sialidase treatment prior to virus infection appreciably enhanced the number of infected cells. We therefore used the virus-containing 293T cell supernatant to infect MDCK II cells that had been pretreated with 200 mU/ml of *Clostridium perfringens* sialidase. Because no cytopathic effect (CPE) was observed, the cell culture supernatant was blindly passaged in MDCK II cells pretreated with sialidase. At passage 5, the inoculated cells showed a CPE, and most cells had detached by day 3 postinoculation. Virus was harvested, and its entire genome was sequenced. Two mutations in the NA-like protein, F144C and T342A (see Fig. 6), were detected. No mutations were found in the other viral RNA segments.

In parallel with the above-described virus passages in MDCK II cells pretreated with sialidase, we found that addition of 20 mU/ml of sialidase to the growth medium of MDCK II cells resulted in efficient H18N11 virus replication with an apparent CPE in the absence of additional mutations. Using these growth conditions, we generated stocks of wild-type (WT) A/flat-faced bat/Peru/033/2010 virus (the H18N11-WT virus) and of viruses possessing one or both of the mutations in the NA-like protein that emerged during blind passages in MDCK II cells (the H18N11-NA-F144C, H18N11-NA-T342A, and H18N11-NA-F144C/T342A viruses); all virus stocks were sequenced before further experiments were carried out.

Growth kinetics of H18N11 viruses in mammalian cell lines. First, we examined the growth kinetics of the viruses in MDCK II cells, commonly used MDCK cells, and human lung adenocarcinoma (Calu-3) cells. Cells were infected with wild-type and mutant H18N11 viruses at a multiplicity of infection (MOI) of 0.01 and incubated at 37°C in the presence or absence of 20 mU/ml of sialidase. The virus titers in the supernatant were measured by using 50% tissue culture infective dose ($TCID_{50}$) assays in MDCK II cells (Fig. 1).

In MDCK II cells without exogenous sialidase, wild-type H18N11 virus replicated to moderate titers of $10^{5.1}$ $TCID_{50}$ at 96 h postinfection (Fig. 1A, solid blue diamonds). The NA-T342A mutation (Fig. 1A, solid green circles) did not enhance the virus titers significantly, whereas the NA-F144C mutation (Fig. 1A, solid purple squares) increased the virus titers by up to 2 log units. The combination of both mutations in the NA-like protein (NA-F144C/T342A; Fig. 1A, solid red triangles) had a synergistic effect and increased the virus titers by more than 3 log units by 48 h postinfection. The addition of exogenous sialidase (Fig. 1A, open symbols and dotted lines) increased the virus titers compared to those in medium without sialidase, although not all differences were statistically significant. Again, the combination of both mutations in the NA-like protein had a greater enhancing effect on the virus titers than either of the single mutations.

In MDCK cells without exogenous sialidase, wild-type H18N11 virus and both single mutants showed limited replication (Fig. 1B), whereas the synergistic effect of the double mutation in the NA-like protein (Fig. 1B, solid red triangle) conferred efficient replication in a cell line that did not support the efficient replication of wild-type H18N11 virus. The addition of exogenous sialidase further increased the virus titers, although the increase was not always at statistically significant levels.

We also tested the growth of the recombinant H18N11 viruses in human Calu-3 cells. Wild-type viruses and the NA-F144C and NA-T342A mutants replicated to moderate titers in the absence of exogenous sialidase (Fig. 1C). The addition of exogenous sialidase resulted in small increases in virus titers, most of which were not statistically significant. Similar to the data obtained in MDCK and MDCK II cells, the H18N11-NA-

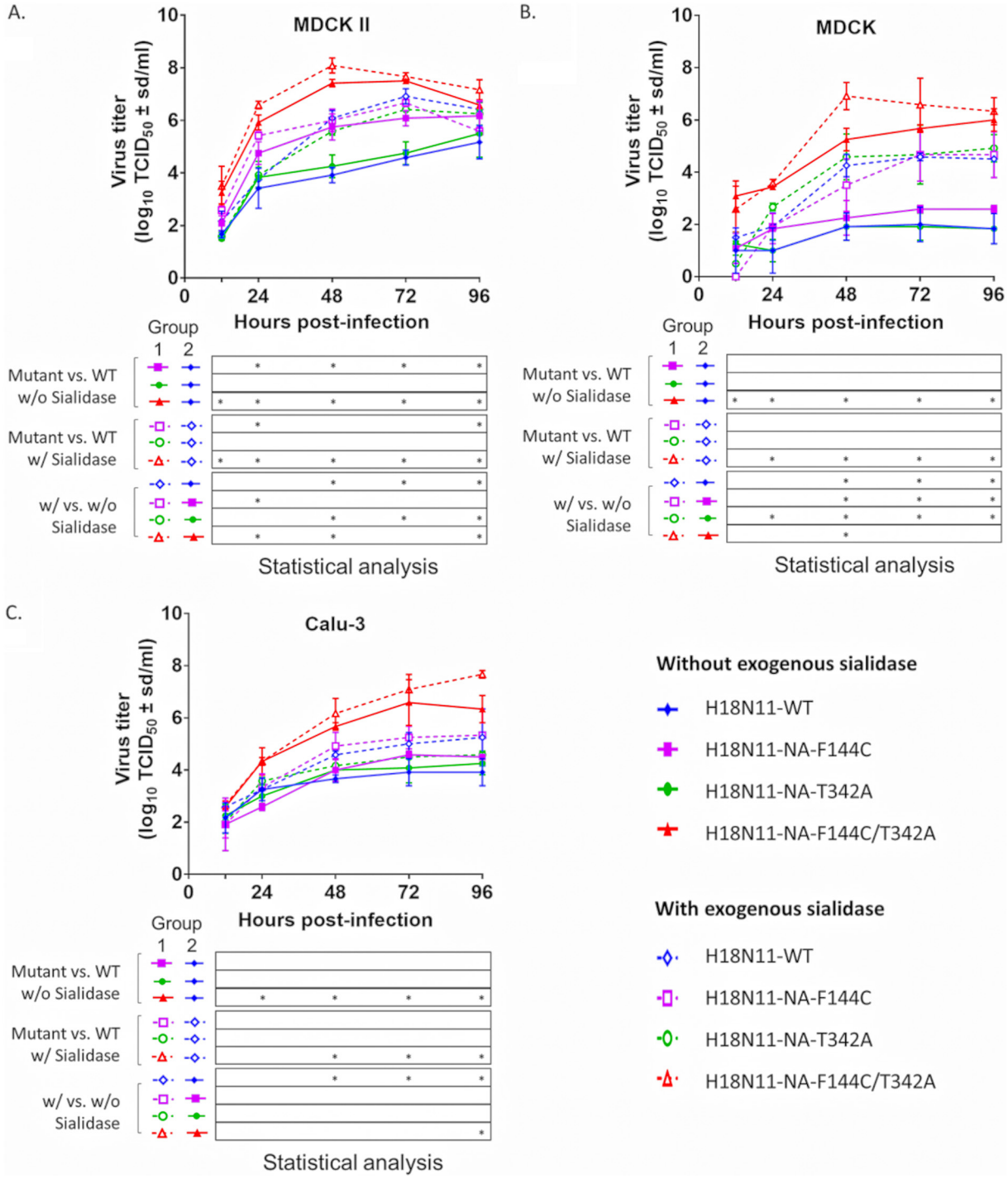

FIG 1 Replication of wild-type and mutant H18N11 viruses in MDCK II, MDCK, and Calu-3 cells in the presence or absence of exogenous sialidase. MDCK II (A), MDCK (B), and Calu-3 (C) cells were infected with wild-type and mutant H18N11 viruses at an MOI of 0.01 for 1 h at 37°C. The cells were then washed with PBS twice and incubated with Opti-MEM medium with 0.5 μg/ml TPCK-trypsin in the presence or absence of sialidase from *Clostridium perfringens* (20 mU/ml). Supernatant was collected at 12, 24, 48, 72, and 96 h for virus titration by use of $TCID_{50}$ assays in MDCK II cells. Virus-infected cells were identified by IFA with an antibody to HA. The data shown are mean values from three independent experiments with standard deviations. *P* values were calculated by use of the R statistical package (www.r-project.org), the lme4 package (47), and the EMMeans package (48), followed by Holm's method (*, $P < 0.05$).

F144C/T342A double mutant displayed notably better replication properties than the wild-type virus and the single mutants.

Virulence of H18N11 viruses in mice. To examine the virulence of the wild-type and mutant H18N11 viruses in mice, groups of 6-week-old female BALB/c mice were

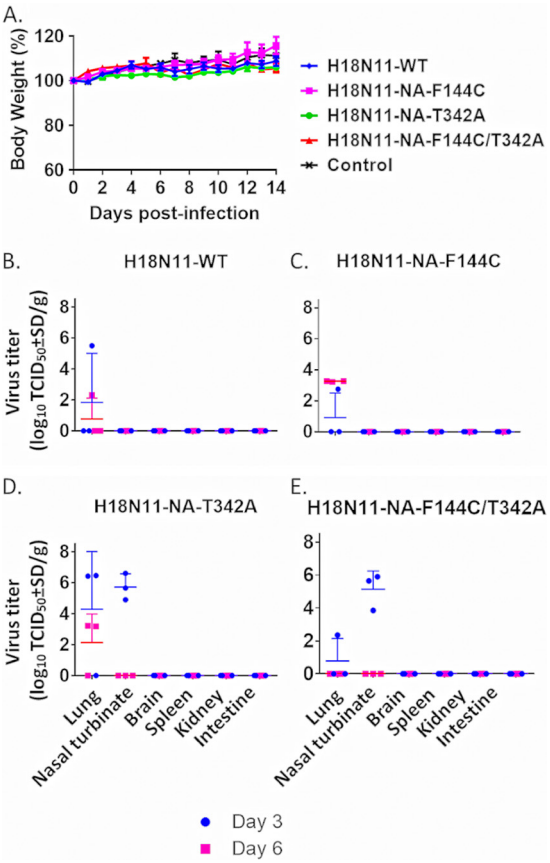

FIG 2 Body weight of and virus replication in mice infected with H18N11 viruses. Nine mice per group were anesthetized and inoculated intranasally with 10^6 $TCID_{50}$/50 μl of wild-type or mutant H18N11 virus. Three mice per group were euthanized on each of days 3 and 6 postinfection, and their lungs, nasal turbinates, brains, spleens, kidneys, and intestines were collected for virus titration (B to E) in MDCK II cells. (A) The remaining three animals per group were monitored for 14 days for body weight changes and signs of disease. The data shown are mean values with standard deviations.

inoculated intranasally with 10^6 $TCID_{50}$ of H18N11 viruses (the H18N11-WT, H18N11-NA-F144C, H18N11-NA-T342A, and H18N11-NA-F144C/T342A viruses). None of the mice lost weight (Fig. 2A) or showed symptoms of illness during the 2 weeks of observation. On each of days 3 and 6 postinoculation, three mice per group were euthanized and organs were collected for virus titration. In mice infected with H18N11-WT, virus was identified in the lungs of one mouse on days 3 and 6 postinfection (Fig. 2B). In the group infected with H18N11-NA-F144C, virus was detected in the lung of one mouse on day 3 postinfection and in the lungs of all three mice on day 6 postinfection (Fig. 2C). Infection with H18N11-NA-T342A led to virus replication in the lungs of two of three infected animals on both day 3 and day 6 postinfection, and infection with H18N11-NA-F144C/T342A led to virus replication in the lungs of one of three infected animals; in addition, relatively high titers of viruses were detected in the nasal turbinates of all three mice on day 3 postinfection (Fig. 2D and E). No virus was detected in the other organs tested; i.e., H18N11 viruses did not replicate systemically in the inoculated mice. These data demonstrate that wild-type H18N11 virus can replicate in the lungs of BALB/c mice, although it does not replicate efficiently. The NA-T342A mutation alone or in combination with the NA-F144C mutation conferred on the virus the ability to replicate in the lower and upper respiratory organs of some of the infected animals.

Virulence of H18N11 viruses in ferrets. To date, the virulence and organ tropism of bat influenza viruses have not been tested in ferrets, animals commonly used as a model in influenza virus research. We therefore intranasally infected groups of six

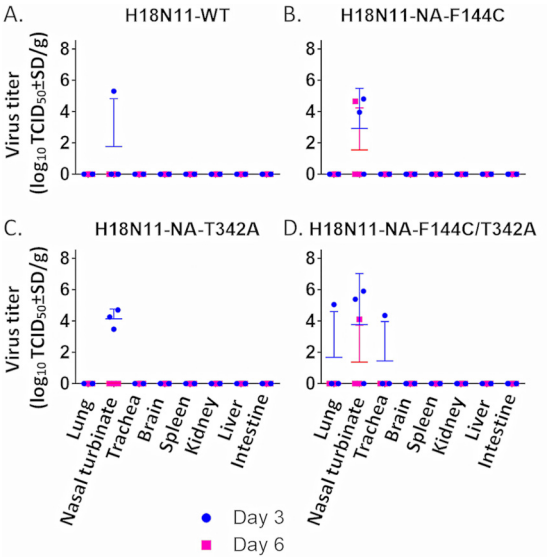

FIG 3 Virus replication in ferrets infected with H18N11 viruses. Six ferrets per group were anesthetized and inoculated intranasally with 10^6 $TCID_{50}$/50 μl of the H18N11-WT (A), H18N11-NA-F144C (B), H18N11-NA-T342A (C), or H18N11-NA-F144C/T342A (D) virus. Three ferrets per group were euthanized on each of days 3 and 6 postinfection, and their lungs, nasal turbinates, tracheas, brains, spleens, kidneys, livers, and intestines were collected for virus titration in MDCK II cells. The data shown are mean values with standard deviations.

6-month-old female ferrets with 10^6 $TCID_{50}$ of viruses (the H18N11-WT, H18N11-NA-F144C, H18N11-NA-T342A, and H18N11-NA-F144C/T342A viruses). Three ferrets from each group were euthanized on each of days 3 and 6 postinfection, and organs were collected for virus titration. Infection with H18N11-WT and single mutant viruses resulted in virus replication in the nasal turbinates of one ferret (an H18N11-WT-infected ferret; Fig. 3A) and three ferrets (H18N11-NA-F144C- and H18N11-NA-T342A-infected ferrets; Fig. 3B and C), respectively. The H18N11-NA-F144C/T342A double mutant was isolated from the nasal turbinates of several animals and also from the lung and trachea of one ferret on day 3 postinfection (Fig. 3D). In two of three infected animals, the infections resolved by day 6 postinfection, and the viruses did not spread to nonrespiratory organs. These data indicate that wild-type H18N11 virus has a limited replicative ability in ferrets and that the combination of the NA-F144C and NA-T342A mutations broadened the tissue tropism in the respiratory tract, with virus replication occurring in the trachea and lung of some, but not all, animals.

Virus morphology and budding. Our data indicated that the mutations in the NA-like protein (which emerged during virus passages in MDCK II cells) increased the replicative ability of the H18N11 virus in cultured cells and extended its tissue tropism in the respiratory tract. To gain insight into the potential role of the mutations in the NA-like protein, we first assessed virus morphology. Influenza A viruses can be spherical, elliptical, or filamentous. Isolates newly isolated from clinical samples tend to be filamentous, whereas laboratory-adapted strains are often spherical or elliptical (34, 35). Here, we observed the morphology of purified H18N11-WT and H18N11-NA-F144C/T342A viruses by use of negative-staining electron microscopy. H18N11-WT virus appeared spherical or elliptical (Fig. 4A), similar to the laboratory-adapted human A/WSN/33 (H1N1) virus (Fig. 4C); however, the glycoprotein spikes on the surface of the virions were less densely packed on bat influenza virions than on A/WSN/33 virions. No significant differences between the morphology of the wild-type virus and that of the NA-F144C/T342A double mutant were observed (Fig. 4B).

The NA protein of conventional influenza A viruses cleaves sialic acids from cellular receptors to prevent the formation of large virus aggregates tethered to host cells, thus facilitating the release of progeny viruses from the infected cells (14–16). However, the

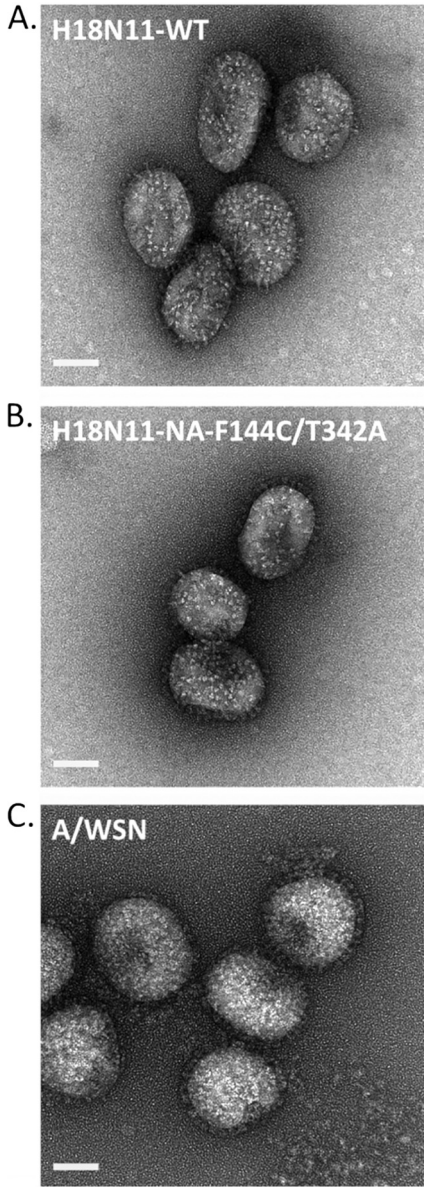

FIG 4 Virus morphology. H18N11-WT (A), H18N11-NA-F144C/T342A (B), and A/WSN/33 (C) viruses were purified, stained with 2% uranyl acetate, and air dried. Virions were observed and representative images were acquired with a Tecnai F20 transmission electron microscope (FEI Company, Eindhoven, Netherlands) at 200 kV. Bars, 50 nm.

NA-like protein of bat influenza viruses lacks sialidase activity (4, 27, 28, 36), and its role in the life cycle of bat influenza viruses is not known. Here, we assessed whether the mutations in the NA-like protein affected the release of budding viruses from infected cells. MDCK II cells were infected with the H18N11-WT and H18N11-NA-F144C/T342A viruses at an MOI of 5 and incubated in the presence or absence of exogenous sialidase. At 14 and 24 h postinfection, cells were fixed, stained, and observed for virus budding by using transmission electron microscopy.

The number of virions released from cells infected with the H18N11-NA-F144C/T342A virus appeared to be higher than the number of virions released from cells infected with the H18N11-WT virus (Fig. 5), consistent with the higher replicative ability of the mutant virus; however, further studies are needed to definitively demonstrate this difference. We did not observe large virus aggregates under any of the conditions tested, suggesting that the mutations in the NA-like protein and/or the exogenous

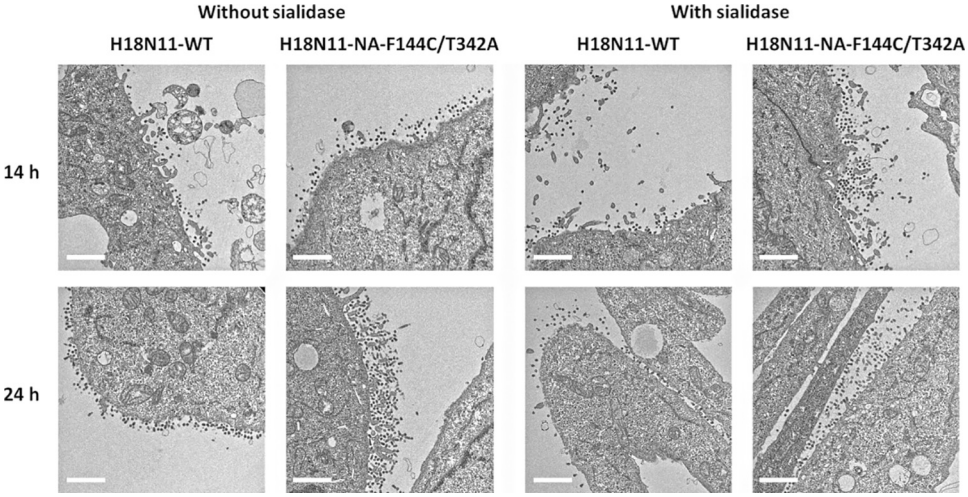

FIG 5 Virus budding observed by use of transmission electron microscopy. MDCK II cells were infected with the H18N11-WT or H18N11-NA-F144C/T342A virus at an MOI of 5. After a 1-h incubation at 37°C, the cells were washed with PBS and Opti-MEM medium with or without 20 mU/ml sialidase was added. At 14 or 24 h postinfection, chemically fixed samples were prepared and ultrathin (110-nm-thick) sections were stained with 2% uranyl acetate and Reynold's lead. Images were acquired with a Tecnai F20 TEM (FEI Company, Eindhoven, the Netherlands) at 200 kV. Bars, 1 μm.

sialidase treatment did not increase the virus titers by preventing the formation of virus aggregates.

DISCUSSION

We generated H18N11 bat influenza virus by reverse genetics and identified mutations in the NA-like protein that emerged during virus passages in cultured cells. These mutations increased the virus titers in cultured cells compared with those in cells infected with the wild-type virus and conferred a tissue tropism broader than that of the wild-type virus in the respiratory tracts of mice and ferrets. However, virus replication was not detected in the lungs and/or nasal turbinates of all infected animals, and no symptoms of disease were observed.

Bat influenza viruses of the H17N10 and H18N11 subtypes were first generated by reverse genetics in 2016 (29), based on sequences extracted from bat tissue samples. Currently, the host range of bat influenza viruses in other mammalian species has not been well studied. Two studies have tested H18N11 virus replication in mice and detected moderate virus titers in the upper airways of C57BL/6J mice infected with the H18N11 virus (26, 37). We found that a reverse genetics-generated H18N11 virus replicated in the lungs of infected BALB/c mice but that the viral titers were low and virus replication was limited to one of three mice euthanized on each of days 3 and 6 postinfection. The less efficient replication of H18N11 in our study may be explained by the different mouse strains used in the two studies. Until recently, bat influenza viruses had not been tested in ferrets. Ciminski et al. (37) tested wild-type H18N11 virus replication in ferrets but were unable to recover virus from any of the organs tested; however, serum conversion was detected in a subset of the infected animals. We detected H18N11 virus replication in the nasal turbinates of one out of six infected animals. Bat influenza virus of the H18N11 subtype can therefore replicate in the respiratory tracts of mice and ferrets but does not cause a severe infection with high titers in different parts of the respiratory tract.

The MDCK II cell-adapted H18N11 virus possessed two mutations in the NA-like protein, F144C and T342A. The genomes of most canonical influenza A viruses of the N1 to N9 subtypes encode a histidine residue at position 144, whereas the genomes of most influenza B viruses encode a tyrosine at this position. The amino acid at position 342 of the NA-like protein is variable among N1 to N9 NA proteins but is conserved in

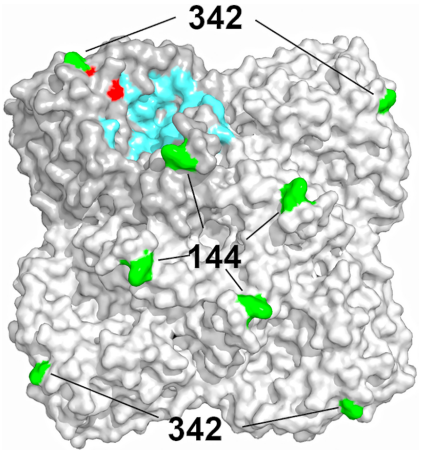

FIG 6 Localization of amino acids NA-144 and NA-342 in the three-dimensional structure of A/flat-faced bat/Peru/033/2010 (H18N11) virus NA-like protein (Protein Data Bank accession number 4MC7). The residues that form the putative catalytic and calcium ion binding sites are shown in blue and red, respectively. The amino acid positions at which mutations emerged during bat virus passages in MDCK II cells are shown in green.

influenza B viruses, in which a glycine is located at this position. In the three-dimensional structure of the N11 NA-like protein (Protein Data Bank accession number 4MC7) (4), residue 144 is located at the outer rim of a pocket, whereas residue 342 is located near the putative calcium ion binding site (Fig. 6). Both of these sites are critical for the sialidase activity of canonical influenza virus NA proteins (38–44).

The N10 and N11 bat influenza NA-like proteins lack sialidase activity, and their function in the bat influenza viral life cycle remains unknown. The NA-F144C/T342A mutations significantly increased the H18N11 virus titers in three different cell lines compared with those achieved with the wild-type virus and supported a tissue tropism in the respiratory tract broader than that supported by the wild-type virus, suggesting a role for the NA-like protein in the bat virus life cycle. We therefore compared the H18N11-WT and H18N11-NA-F144C/T342A viruses with respect to their morphology and efficiency of virion release from infected cells. No significant differences in morphology were observed between the wild-type and mutant bat viruses. In addition, no large virus aggregates formed with the wild-type NA-like protein in the absence of exogenous sialidase, which could explain the need for exogenous sialidase and/or mutations in the NA-like protein to enable the efficient release of single virions. Thus, the exact role of the bat influenza virus NA-like protein and the NA-F144C/T342A mutations in the bat influenza virus life cycle remains in question.

MATERIALS AND METHODS

Cells. Madin-Darby canine kidney subclone II (MDCK II) and subclone 2 (MDCK.2) cells were purchased from the European Collection of Authenticated Cell Cultures (ECACC) and the American Type Culture Collection (ATCC), respectively, and maintained in minimum essential medium (MEM) containing 10% fetal bovine serum (FBS) and antibiotics. Madin-Darby canine kidney (MDCK) cells were obtained from ATCC. MDCK cells were maintained in MEM containing 5% newborn calf serum, essential amino acids, vitamins, and antibiotics. Human embryonic kidney (293T) cells and human lung adenocarcinoma (Calu-3) cells were obtained from ATCC and maintained in Dulbecco's modified Eagle's medium containing 10% FBS and antibiotics. All cells were incubated at 37°C with 5% CO_2.

Plasmids and reverse genetics. Viral cDNA of A/flat-faced bat/Peru/033/2010 (H18N11) virus was cloned into the pHH21 vRNA transcription plasmid between the human RNA polymerase I promoter and the mouse RNA polymerase I terminator (30). Mutations in the NA-like protein were introduced by site-directed mutagenesis PCR. Viral cDNAs of the PB2, PB1, PA, and NP segments were cloned into a eukaryotic protein expression plasmid (pCAGGS) under the control of the chicken β-actin promoter (31). All plasmids were mixed and cotransfected into 293T cells by using the TransIT-293 reagent (Mirus, Madison, WI). The supernatant containing infectious virus was harvested at 48 h posttransfection and amplified as described below.

Viruses. To amplify the reverse genetics-generated A/flat-faced bat/Peru/033/2010 (H18N11) virus, MDCK II cells were pretreated with 200 mU/ml of sialidase from *Clostridium perfringens* (MilliporeSigma,

St. Louis, MO, USA) diluted in phosphate-buffered saline (PBS) at 37°C for 1 h. After sialidase pretreatment, MDCK II cells were infected with virus-containing 293T cell supernatant (see the previous paragraph) and passaged five times in sialidase-pretreated MDCK II cells. The recovered virus was sequenced by Sanger sequencing and found to possess two mutations in the NA-like protein (F144C and T342A). Therefore, we regenerated the virus by reverse genetics and amplified it in MDCK II cells with Opti-MEM medium (Thermo Fisher, Waltham, MA, USA) and 0.5 μg/ml TPCK (tosylsulfonyl phenylalanyl chloromethyl ketone)-trypsin (Worthington, Lakewood, NJ, USA); here, we added the sialidase (20 mU/ml) to the growth medium, which resulted in efficient virus replication without the emergence of adapting mutations. Virus titers were determined by use of $TCID_{50}$ assays in MDCK II cells. Positive wells were observed by using an immunofluorescent assay (IFA) with a monoclonal antibody (CR9114) to HA (45).

Immunofluorescent assay (IFA). MDCK II cells infected with the H18N11 virus were fixed with 4% paraformaldehyde (Electron Microscopy Sciences, Hatfield, PA, USA) in PBS at room temperature for 15 min and incubated with 10% normal goat serum (Thermo Fisher, Waltham, MA, USA) in PBS to block nonspecific binding. The cells were then incubated with a humanized monoclonal antibody (CR9114) to HA (45) for 1 h. After three washes with PBS, the cells were incubated with Alexa Fluor 488-conjugated goat anti-human IgG (Thermo Fisher, Waltham, MA, USA). Fluorescence was observed under an Evos fluorescence microscope (Thermo Fisher, Waltham, MA, USA).

Virus growth kinetics. MDCK II, MDCK, and Calu-3 cells were infected with virus at a multiplicity of infection (MOI) of 0.01. After a 1-h incubation at 37°C, the cells were washed twice with PBS and Opti-MEM medium with 0.5 μg/ml TPCK-trypsin with or without 20 mU/ml of sialidase was added. Supernatants were collected at 12, 24, 48, 72, and 96 h postinfection and titrated in MDCK II cells by using $TCID_{50}$ assays.

Mouse experiments. Groups of nine 6-week-old female BALB/c mice (The Jackson Laboratory, Bar Harbor, ME) were anesthetized with isoflurane and inoculated intranasally with 10^6 $TCID_{50}$/50 μl of wild-type or mutant H18N11 virus. On each of days 3 and 6 postinoculation, three mice per group were euthanized and their organs (lung, nasal turbinates, brain, spleen, kidney, and intestine) were collected for virus titration. The remaining three animals per group were monitored for 14 days for weight loss and signs of disease. Project protocols for animal use were carried out at the University of Wisconsin—Madison under animal protocol number V00806.

Ferret experiments. Groups of six 6-month-old female ferrets (Triple F Farms, Sayre, PA, USA) were inoculated intranasally with 10^6 $TCID_{50}$/500 μl of virus. On each of days 3 and 6 postinoculation, three ferrets were euthanized and their organs (lungs, tracheas, nasal turbinates, brains, spleens, kidneys, livers, and intestines) were collected for virus titration.

Negative-staining electron microscopy to assess virus morphology. Viruses were purified and stained with 2% uranyl acetate and air dried as described previously (46). Virions were observed and representative images were acquired with a Tecnai F20 transmission electron microscope (TEM; FEI Company, Eindhoven, Netherlands) at 200 kV.

Transmission electron microscopy to assess virus budding. MDCK II cells were infected with virus at an MOI of 5. After a 1-h incubation at 37°C, the cells were washed with PBS and Opti-MEM medium with or without 20 mU/ml sialidase was added. At 14 and 24 h postinfection, chemically fixed samples were prepared as previously described (46). Ultrathin (110-nm-thick) sections were stained with 2% uranyl acetate and Reynold's lead. The images were acquired with a Tecnai F20 TEM (FEI Company, Eindhoven, the Netherlands) at 200 kV.

Statistical analysis. For the analysis of viral growth curves, we performed a linear mixed-effects analysis. As fixed effects, we used the viruses and the time point of the measurement (with an interaction term between those fixed effects). As random effects, we used the intercepts of the individual replicates. We transformed the virus titer values to the $\log_{10}$ scale and used the R statistical package (www.r-project.org), the lme4 package (47), and the EMMeans package (version 1.2.4) for the group comparisons; *P* values were adjusted using Holm's method. A similar analysis was used for the animal weight loss data.

For the comparison of virus titers in animal organs, we used unpaired two-sided *t* tests at each time point separately when comparing only two samples. For comparisons involving multiple samples, we used a one-way analysis of variance, followed by Tukey's honestly significant difference *post hoc* test.

In all statistical analyses, we considered the differences significant if the *P* values were <0.05.

Biosafety. All recombinant DNA protocols were approved by the University of Wisconsin—Madison Institutional Biosafety Committee, after risk assessments were conducted by the Office of Biological Safety. All experiments were approved by the University of Wisconsin—Madison Institutional Biosafety Committee. The manuscript was reviewed by the University of Wisconsin—Madison Dual Use Research of Concern (DURC) Subcommittee. The review was conducted in accordance with the September 2014 DURC policy of the U.S. government. The University of Wisconsin DURC Subcommittee concluded that the studies described herein are not DURC. In addition, the University of Wisconsin—Madison Biosecurity Task Force regularly reviews the research, policies, and practices of research conducted with pathogens of high consequence at the institution. This task force has a diverse skill set and provides support in the areas of biosafety, facilities, compliance, security, law, and health. Members of the Biosecurity Task Force are in frequent contact with the principal investigators and laboratory personnel to provide oversight and ensure biosecurity. All experiments with infectious bat H18N11 influenza viruses were performed in a biosafety level 3 (BSL3) containment laboratory.

ACKNOWLEDGMENTS

We thank Susan Watson for scientific editing.

Part of this work was supported by the Center for Research on Influenza Pathogenesis (CRIP; grant HHSN272201400008C) and by the Japan Initiative for Global Research Network on Infectious Diseases (J-GRID) from the Japan Agency for Medical Research and Development (AMED; grant JP19fm0108006).

REFERENCES

1. Fouchier RA, Munster V, Wallensten A, Bestebroer TM, Herfst S, Smith D, Rimmelzwaan GF, Olsen B, Osterhaus AD. 2005. Characterization of a novel influenza A virus hemagglutinin subtype (H16) obtained from black-headed gulls. J Virol 79:2814–2822. https://doi.org/10.1128/JVI.79.5.2814-2822.2005.
2. Webster RG, Bean WJ, Gorman OT, Chambers TM, Kawaoka Y. 1992. Evolution and ecology of influenza A viruses. Microbiol Rev 56:152–179.
3. Tong S, Li Y, Rivailler P, Conrardy C, Castillo DA, Chen LM, Recuenco S, Ellison JA, Davis CT, York IA, Turmelle AS, Moran D, Rogers S, Shi M, Tao Y, Weil MR, Tang K, Rowe LA, Sammons S, Xu X, Frace M, Lindblade KA, Cox NJ, Anderson LJ, Rupprecht CE, Donis RO. 2012. A distinct lineage of influenza A virus from bats. Proc Natl Acad Sci U S A 109:4269–4274. https://doi.org/10.1073/pnas.1116200109.
4. Tong S, Zhu X, Li Y, Shi M, Zhang J, Bourgeois M, Yang H, Chen X, Recuenco S, Gomez J, Chen LM, Johnson A, Tao Y, Dreyfus C, Yu W, McBride R, Carney PJ, Gilbert AT, Chang J, Guo Z, Davis CT, Paulson JC, Stevens J, Rupprecht CE, Holmes EC, Wilson IA, Donis RO. 2013. New World bats harbor diverse influenza A viruses. PLoS Pathog 9:e1003657. https://doi.org/10.1371/journal.ppat.1003657.
5. Zhou B, Ma JJ, Liu QF, Bawa B, Wang W, Shabman RS, Duff M, Lee J, Lang YK, Cao N, Nagy A, Lin XD, Stockwell TB, Richt JA, Wentworth DE, Ma WJ. 2014. Characterization of uncultivable bat influenza virus using a replicative synthetic virus. PLoS Pathog 10:e1004420. https://doi.org/10.1371/journal.ppat.1004420.
6. Juozapaitis M, Aguiar Moreira E, Mena I, Giese S, Riegger D, Pohlmann A, Hoper D, Zimmer G, Beer M, Garcia-Sastre A, Schwemmle M. 2014. An infectious bat-derived chimeric influenza virus harbouring the entry machinery of an influenza A virus. Nat Commun 5:4448. https://doi.org/10.1038/ncomms5448.
7. Tefsen B, Lu G, Zhu Y, Haywood J, Zhao L, Deng T, Qi J, Gao GF. 2014. The N-terminal domain of PA from bat-derived influenza-like virus H17N10 has endonuclease activity. J Virol 88:1935–1941. https://doi.org/10.1128/JVI.03270-13.
8. Zhao X, Tefsen B, Li Y, Qi J, Lu G, Shi Y, Yan J, Xiao H, Gao GF. 2016. The NS1 gene from bat-derived influenza-like virus H17N10 can be rescued in influenza A PR8 backbone. J Gen Virol 97:1797–1806. https://doi.org/10.1099/jgv.0.000509.
9. Turkington HL, Juozapaitis M, Tsolakos N, Corrales-Aguilar E, Schwemmle M, Hale BG. 2018. Unexpected functional divergence of bat influenza virus NS1 proteins. J Virol 92:e02097-17. https://doi.org/10.1128/JVI.02097-17.
10. Yang J, Lee J, Ma J, Lang Y, Nietfeld J, Li Y, Duff M, Li Y, Yang Y, Liu H, Zhou B, Wentworth DE, Richt JA, Li Z, Ma W. 2017. Pathogenicity of modified bat influenza virus with different M genes and its reassortment potential with swine influenza A virus. J Gen Virol 98:577–584. https://doi.org/10.1099/jgv.0.000715.
11. Rogers GN, Paulson JC. 1983. Receptor determinants of human and animal influenza virus isolates: differences in receptor specificity of the H3 hemagglutinin based on species of origin. Virology 127:361–373. https://doi.org/10.1016/0042-6822(83)90150-2.
12. Shinya K, Ebina M, Yamada S, Ono M, Kasai N, Kawaoka Y. 2006. Avian flu: influenza virus receptors in the human airway. Nature 440:435–436. https://doi.org/10.1038/440435a.
13. Yamada S, Suzuki Y, Suzuki T, Le MQ, Nidom CA, Sakai-Tagawa Y, Muramoto Y, Ito M, Kiso M, Horimoto T, Shinya K, Sawada T, Kiso M, Usui T, Murata T, Lin Y, Hay A, Haire LF, Stevens DJ, Russell RJ, Gamblin SJ, Skehel JJ, Kawaoka Y. 2006. Haemagglutinin mutations responsible for the binding of H5N1 influenza A viruses to human-type receptors. Nature 444:378–382. https://doi.org/10.1038/nature05264.
14. Air GM, Laver WG. 1989. The neuraminidase of influenza virus. Proteins 6:341–356. https://doi.org/10.1002/prot.340060402.
15. Moscona A. 2005. Neuraminidase inhibitors for influenza. N Engl J Med 353:1363–1373. https://doi.org/10.1056/NEJMra050740.
16. Palese P, Tobita K, Ueda M, Compans RW. 1974. Characterization of temperature sensitive influenza virus mutants defective in neuraminidase. Virology 61:397–410. https://doi.org/10.1016/0042-6822(74)90276-1.
17. Mitnaul LJ, Matrosovich MN, Castrucci MR, Tuzikov AB, Bovin NV, Kobasa D, Kawaoka Y. 2000. Balanced hemagglutinin and neuraminidase activities are critical for efficient replication of influenza A virus. J Virol 74:6015–6020. https://doi.org/10.1128/jvi.74.13.6015-6020.2000.
18. Rudneva IA, Kovaleva VP, Varich NL, Farashyan VR, Gubareva LV, Yamnikova SS, Popova IA, Presnova VP, Kaverin NV. 1993. Influenza A virus reassortants with surface glycoprotein genes of the avian parent viruses: effects of HA and NA gene combinations on virus aggregation. Arch Virol 133:437–450. https://doi.org/10.1007/bf01313781.
19. Rudneva IA, Sklyanskaya EI, Barulina OS, Yamnikova SS, Kovaleva VP, Tsvetkova IV, Kaverin NV. 1996. Phenotypic expression of HA-NA combinations in human-avian influenza A virus reassortants. Arch Virol 141:1091–1099. https://doi.org/10.1007/bf01718612.
20. Gubareva LV, Bethell R, Hart GJ, Murti KG, Penn CR, Webster RG. 1996. Characterization of mutants of influenza A virus selected with the neuraminidase inhibitor 4-guanidino-Neu5Ac2en. J Virol 70:1818–1827.
21. Hughes MT, Matrosovich M, Rodgers ME, McGregor M, Kawaoka Y. 2000. Influenza A viruses lacking sialidase activity can undergo multiple cycles of replication in cell culture, eggs, or mice. J Virol 74:5206–5212. https://doi.org/10.1128/jvi.74.11.5206-5212.2000.
22. McKimm-Breschkin JL, Blick TJ, Sahasrabudhe A, Tiong T, Marshall D, Hart GJ, Bethell RC, Penn CR. 1996. Generation and characterization of variants of NWS/G70C influenza virus after in vitro passage in 4-amino-Neu5Ac2en and 4-guanidino-Neu5Ac2en. Antimicrob Agents Chemother 40:40–46. https://doi.org/10.1128/AAC.40.1.40.
23. Xu R, Zhu X, McBride R, Nycholat CM, Yu W, Paulson JC, Wilson IA. 2012. Functional balance of the hemagglutinin and neuraminidase activities accompanies the emergence of the 2009 H1N1 influenza pandemic. J Virol 86:9221–9232. https://doi.org/10.1128/JVI.00697-12.
24. Yen HL, Liang CH, Wu CY, Forrest HL, Ferguson A, Choy KT, Jones J, Wong DD, Cheung PP, Hsu CH, Li OT, Yuen KM, Chan RW, Poon LL, Chan MC, Nicholls JM, Krauss S, Wong CH, Guan Y, Webster RG, Webby RJ, Peiris M. 2011. Hemagglutinin-neuraminidase balance confers respiratory-droplet transmissibility of the pandemic H1N1 influenza virus in ferrets. Proc Natl Acad Sci U S A 108:14264–14269. https://doi.org/10.1073/pnas.1111000108.
25. Sun X, Shi Y, Lu X, He J, Gao F, Yan J, Qi J, Gao GF. 2013. Bat-derived influenza hemagglutinin H17 does not bind canonical avian or human receptors and most likely uses a unique entry mechanism. Cell Rep 3:769–778. https://doi.org/10.1016/j.celrep.2013.01.025.
26. Karakus U, Thamamongood T, Ciminski K, Ran W, Gunther SC, Pohl MO, Eletto D, Jeney C, Hoffmann D, Reiche S, Schinkothe J, Ulrich R, Wiener J, Hayes MGB, Chang MW, Hunziker A, Yanguez E, Aydillo T, Krammer F, Oderbolz J, Meier M, Oxenius A, Halenius A, Zimmer G, Benner C, Hale BG, Garcia-Sastre A, Beer M, Schwemmle M, Stertz S. 2019. MHC class II proteins mediate cross-species entry of bat influenza viruses. Nature 567:109–112. https://doi.org/10.1038/s41586-019-0955-3.
27. Zhu X, Yang H, Guo Z, Yu W, Carney PJ, Li Y, Chen LM, Paulson JC, Donis RO, Tong S, Stevens J, Wilson IA. 2012. Crystal structures of two subtype N10 neuraminidase-like proteins from bat influenza A viruses reveal a diverged putative active site. Proc Natl Acad Sci U S A 109:18903–18908. https://doi.org/10.1073/pnas.1212579109.
28. Li Q, Sun X, Li Z, Liu Y, Vavricka CJ, Qi J, Gao GF. 2012. Structural and functional characterization of neuraminidase-like molecule N10 derived from bat influenza A virus. Proc Natl Acad Sci U S A 109:18897–18902. https://doi.org/10.1073/pnas.1211037109.
29. Moreira EA, Locher S, Kolesnikova L, Bolte H, Aydillo T, Garcia-Sastre A,

Schwemmle M, Zimmer G. 2016. Synthetically derived bat influenza A-like viruses reveal a cell type- but not species-specific tropism. Proc Natl Acad Sci U S A 113:12797–12802. https://doi.org/10.1073/pnas.1608821113.
30. Neumann G, Watanabe T, Ito H, Watanabe S, Goto H, Gao P, Hughes M, Perez DR, Donis R, Hoffmann E, Hobom G, Kawaoka Y. 1999. Generation of influenza A viruses entirely from cloned cDNAs. Proc Natl Acad Sci U S A 96:9345–9350. https://doi.org/10.1073/pnas.96.16.9345.
31. Niwa H, Yamamura K, Miyazaki J. 1991. Efficient selection for high-expression transfectants with a novel eukaryotic vector. Gene 108:193–199. https://doi.org/10.1016/0378-1119(91)90434-d.
32. Hansson GC, Simons K, van Meer G. 1986. Two strains of the Madin-Darby canine kidney (MDCK) cell line have distinct glycosphingolipid compositions. EMBO J 5:483–489. https://doi.org/10.1002/j.1460-2075.1986.tb04237.x.
33. Dukes JD, Whitley P, Chalmers AD. 2011. The MDCK variety pack: choosing the right strain. BMC Cell Biol 12:43. https://doi.org/10.1186/1471-2121-12-43.
34. Chu CM, Dawson IM, Elford WJ. 1949. Filamentous forms associated with newly isolated influenza virus. Lancet i:602. https://doi.org/10.1016/s0140-6736(49)91699-2.
35. Kilbourne ED, Murphy JS. 1960. Genetic studies of influenza viruses. I. Viral morphology and growth capacity as exchangeable genetic traits. Rapid in ovo adaptation of early passage Asian strain isolates by combination with PR8. J Exp Med 111:387–406. https://doi.org/10.1084/jem.111.3.387.
36. Garcia-Sastre A. 2012. The neuraminidase of bat influenza viruses is not a neuraminidase. Proc Natl Acad Sci U S A 109:18635–18636. https://doi.org/10.1073/pnas.1215857109.
37. Ciminski K, Ran W, Gorka M, Lee J, Malmlov A, Schinkothe J, Eckley M, Murrieta RA, Aboellail TA, Campbell CL, Ebel GD, Ma J, Pohlmann A, Franzke K, Ulrich R, Hoffmann D, Garcia-Sastre A, Ma W, Schountz T, Beer M, Schwemmle M. 2019. Bat influenza viruses transmit among bats but are poorly adapted to non-bat species. Nat Microbiol 4:2298–2309. https://doi.org/10.1038/s41564-019-0556-9.
38. Smith BJ, Huyton T, Joosten RP, McKimm-Breschkin JL, Zhang JG, Luo CS, Lou MZ, Labrou NE, Garrett TP. 2006. Structure of a calcium-deficient form of influenza virus neuraminidase: implications for substrate binding. Acta Crystallogr D Biol Crystallogr 62:947–952. https://doi.org/10.1107/S0907444906020063.
39. Burmeister WP, Cusack S, Ruigrok R. 1994. Calcium is needed for the thermostability of influenza B virus neuraminidase. J Gen Virol 75:381–388. https://doi.org/10.1099/0022-1317-75-2-381.
40. Chong AK, Pegg MS, Taylor NR, von Itzstein M. 1992. Evidence for a sialosyl cation transition-state complex in the reaction of sialidase from influenza virus. Eur J Biochem 207:335–343. https://doi.org/10.1111/j.1432-1033.1992.tb17055.x.
41. Varghese JN, Colman PM, van Donkelaar A, Blick TJ, Sahasrabudhe A, McKimm-Breschkin JL. 1997. Structural evidence for a second sialic acid binding site in avian influenza virus neuraminidases. Proc Natl Acad Sci U S A 94:11808–11812. https://doi.org/10.1073/pnas.94.22.11808.
42. Colman PM, Varghese JN, Laver WG. 1983. Structure of the catalytic and antigenic sites in influenza virus neuraminidase. Nature 303:41–44. https://doi.org/10.1038/303041a0.
43. Varghese JN, Laver WG, Colman PM. 1983. Structure of the influenza virus glycoprotein antigen neuraminidase at 2.9 Å resolution. Nature 303:35–40. https://doi.org/10.1038/303035a0.
44. Varghese JN, Colman PM. 1991. Three-dimensional structure of the neuraminidase of influenza virus A/Tokyo/3/67 at 2.2 Å resolution. J Mol Biol 221:473–486. https://doi.org/10.1016/0022-2836(91)80068-6.
45. Yamayoshi S, Uraki R, Ito M, Kiso M, Nakatsu S, Yasuhara A, Oishi K, Sasaki T, Ikuta K, Kawaoka Y. 2017. A broadly reactive human anti-hemagglutinin stem monoclonal antibody that inhibits influenza A virus particle release. EBioMedicine 17:182–191. https://doi.org/10.1016/j.ebiom.2017.03.007.
46. Nakatsu S, Murakami S, Shindo K, Horimoto T, Sagara H, Noda T, Kawaoka Y. 2018. Influenza C and D viruses package eight organized ribonucleoprotein complexes. J Virol 92:e02084-17. https://doi.org/10.1128/JVI.02084-17.
47. Bates D, Machler M, Bolker BM, Walker SC. 2015. Fitting linear mixed-effects models using lme4. J Stat Soft 67:1–48. https://doi.org/10.18637/jss.v067.i01.
48. Lenth R. 2018. EMMeans: estimated marginal means, aka least-squares means. R package version 1.2.4. https://CRAN.R-project.org/package=emmeans.